

Zn-Porphyrin Nanoring as a CO Gas Sensor: A Fast Response and Short Recovery Time Sensor

Arshadi, Sattar*[†]; Abdolazadeh, Fatemeh; Vessally, Esmail

Department of Chemistry, Payame Noor University, Tehran, I.R. IRAN

ABSTRACT: The butadiyne-linked four-metalloporphyrin nanoring (Zn4P4) is a promising candidate in future nanoelectronic applications such as nanosensors for small gas molecules. The aim of this work is to analyze the CO gas sensing capacity of Zn4P4 using Density Functional Theory (DFT) calculations at CAM-B3LYP/6-31G (d,p) level of theory. To predict the gas adsorption properties of the Zn4P4 system the geometrical structures, binding energies, band gaps, the Density of States (DOS), adsorption energies (E_{ads}^{BSSE}), HOMO and LUMO energies, Fermi level energies (E_{FL}), Natural Bond Orbital (NBO), and Frontier Molecular Orbital (FMO) were calculated. Here it should be remarked that the adsorption of CO gas molecule on Zn4P4 nanoring from the outer side is higher than the inner side. Moreover, the adsorption from the Carbon site of the CO gas molecule is stronger than from the Oxygen site. Also, the closest distance of CO with the Zn4P4 molecule is in the range of 2.505-2.706 Å. Moreover, the range of E_{ads}^{BSSE} values was from -6.50 to -9.40 kCal/mol. The results revealed that during the adsorption of CO gas molecule on Zn4P4 the amounts of E_g and consequently, σ have been considerably changed. Based on the calculated E_{ads}^{BSSE} and a notable decrease in the E_g , it is expected that the Zn4P4 is sensitive to CO molecules. Amazingly, the Zn4P4-CO records favorable values of recovery times for different attempt frequencies. Therefore, the results open a way for the development of a new and selective CO nanosensor.

KEYWORDS: Zn-Porphyrin Nanoring; Selective CO Sensor; Recovery Time; Adsorption.

INTRODUCTION

Carbon monoxide (CO) is an odorless, toxic gas that harms humans due to its high binding ability with hemoglobin. Because of that, in order to reduce environmental pollution and health risk, it is necessary to use methods and techniques to detect this gas and commercialize them in the form of CO sensors [1].

Recently, alkyne-linked π -conjugated metalloporphyrin oligomers have drawn much attention as artificial light-harvesting and photosynthetic antennae [2]. The primary

attention in these systems arose as the role of porphyrin rings as building blocks in biological macromolecules such as hemoglobin and chlorophyll was well-known.

Porphyrins are a group of heterocyclic macrocycle compounds containing a large π -conjugated system formed by four pyrrole subunits interconnected via methine bridges with unique biochemical properties [3]. Linear conjugated porphyrin oligomers show strong long-range electronic coupling [4] and rich nonlinear optical

* To whom correspondence should be addressed.

† E-mail: chemistry_arshadi@pnu.ac.ir

1021-9986/2022/3/754-766

13/\$/6.03

behavior [5], so providing a drive for the synthesis of cyclic conjugated porphyrin oligomers. Porphyrin units are connected with a various number of linking carbon atoms or “fused”, i.e. with no linker which greatly affects the electronic properties of cyclic porphyrin oligomers [6]. The cyclic supramolecular structures with large fully π -conjugated porphyrin arrays were synthesized and characterized including the nanorings, the hierarchical ring in ring assemblies such as Russian doll complexes [7], the discrete π -conjugated metal porphyrin nanotubes, the directly fused tetrameric porphyrin sheets [8] and the porphyrin nano balls [9]. The large butadiyne-linked π -conjugated metalloporphyrin nanorings have attracted particular attention because of their structural, electronic, and topological features, which make them proper nominees for light-harvesting applications [10].

Recently, the study of template-bound metalloporphyrin nanorings has attracted much attention. These may be generated either as a direct product of synthesis, where the template acts as a framework for the coupling of porphyrin subunits [11] or *via* the addition of an excess of molecules to a solution of the free nanoring [12]. Despite the role of templates as scaffolding in the synthesis process, their complex with nanorings has noteworthy structural and dynamical properties in their own right, specifically in boosting the stabilization of novel ring conformations. The growing fascination with these structures arises from the fact that the templates lead rigidity into the otherwise flexible nanorings, leading to fully conjugated cyclic porphyrin frameworks which may be shape-persistent in solution.

Regarding the novelty of this paper, it can be stated that the DFT theoretical studies used to describe the adsorption behavior of the CO gas molecule on butadiyne-linked 4-Zn-porphyrin nanoring has not been considered in previous studies. Our aim is to characterize the 4-Zn-porphyrin nanoring (Zn4P4) and thus explore the possibility of the Zn4P4 as CO gas sensor. The frontier molecular orbital (FMO) [13], the Density of State (DOS), and the Natural Bond Orbital (NBO) [14] were analyzed to understand the sensing mechanism of Zn4P4 upon such gaseous species. Definitely, the obtained results shed light on a comprehensive understanding of Zn4P4 as a selective and sensitive sensor of CO gas which could provide some guidance to the experimentalists in the near future to realize its application [15,16].

THEORETICAL SECTION

Computational methods

In order to study the structural parameters and electronic properties of the Zn4P4 as CO, gas sensor, the DFT calculations were carried out. The equilibrium geometries, adsorption energies, FMO, and Density of State (DOS) analyses were done for these complexes. All calculations were performed using GAMESS software [17] at the level of CAM-B3LYP/ 6-31G (d,p). The relaxed structures were further subjected to the computations for harmonic vibrational frequencies in order to be aware of and validate the actual minimization. The basis set superposition error (BSSE) for the adsorption energy was corrected using BSSE correction through the counterpoise method with “ghost” atoms [18] according to the following equation:

$$E_{\text{ads}}^{\text{BSSE}} = E_{\text{Zn4P4/gas}} - \left(E_{\text{Zn4P4/gas ghost}} + E_{\text{gas/Zn4P4 ghost}} \right)$$

Where the $E_{\text{ads}}^{\text{BSSE}}$ is the BSSE-corrected adsorption energy. The “ghost” atoms correspond to additional basis wave functions centered at the position of the gas and the Zn4P4 without any atomic potential.

The E_g is the energy gap between HOMO which is calculated using $E_g = E_{\text{LUMO}} - E_{\text{HOMO}}$ equation.

The work function ($\Phi = E_{\infty} - E_F$) can be defined as the minimum quantity of energy needed to separate an electron from the Fermi level (E_F) to a point far enough not to sense any efficacy (E_{∞}). It can be said that the Fermi level in a molecule at $T = 0$ K is located nearly in the middle of the HOMO-LUMO gap [19]. The variation of the work function of an adsorbent during the gas adsorption process changes its field emission characteristics which can be monitored via suspended gate field-effect machines [20]. Subsequently, the equation $j = AT^2 \exp(-\Phi/KT)$ describes the current densities of an emitted electron in a vacuum. In this equation, A ($A/K^2.m^2$), T (K), and Φ (eV) were defined as the Richardson constant, temperature, and work function, respectively.

According to the Koopmans theorem [21], chemical hardness (η) can be approximated by $\eta = -1/2(I-A)$ equation. Chemical potential (μ) is described according to $\mu = -\chi = -1/2(I+A)$ equation. In these equations, χ ($-\mu$), I ($-E_{\text{HOMO}}$), and A ($-E_{\text{LUMO}}$) are defined as the electronegativity, ionization potential, and electron affinity of the molecule, respectively.

Electrophilicity index ($\omega = \mu^2/2\eta$) which was stated for the first time by Parr *et. al.* [22] and also Softness ($S = 1/2\eta$) were determined.

The amount of charge transfer between the gas molecules (A) and Zn4P4 (B) was calculated using the $\Delta N = (\mu_B - \mu_A) / 2(\eta_A + \eta_B)$. A positive value of ΔN shows that charge flows from B to A and A act as an electron acceptor [23].

In order to study the stabilization energies of donor-acceptor orbitals and obtain the charge transfer energy, the natural bonding orbital (NBO) calculations were done on all optimized structures [24].

RESULTS AND DISCUSSION

Primarily, the accuracy of the applied method was analyzed to understand the relative stability of the studied compounds. The calculated binding energies (E_b) of butadiyne-linked four-porphyrin nanoring (P₄; C₉₆H₄₀N₁₆) and butadiyne-linked four-metalloporphyrin nanoring (Zn4P₄; C₉₆H₄₀N₁₆Zn₄) are -6.22 and -7.96 eV, respectively. The negative values of E_b revealed that the studied compounds are stable [25].

In this research, the adsorption of CO gas molecules through Zn4P₄ was investigated by using DFT calculations. At first, all the studied structures were optimized in order to get a structure with minimum energy. After optimization of all primary structures including P₄ and Zn4P₄, gotten data was used for comparing electronic and structural properties after adsorption of mentioned gases.

Effect of Zn²⁺ ion adsorption on the electronic properties of P₄

The Zn4P₄ is a porphyrin nanoring with four porphyrins (P₄) that were linked together by 1,3-Butadiyne bridges, and four Zn²⁺ ions localized in the center of porphyrin rings. It should be noted that since P₄ has 8 negative charges on nitrogen atoms of porphyrins so, the whole system (Zn4P₄) is neutral.

The adsorption energy of 4 Zn²⁺, inserted in the porphyrins cavity of P₄, was -229.10 eV (Fig. 1 and Table 1) and indicated a desirable and exothermic process. Hence, the chemisorption of Zn²⁺ ions into P₄ is very strong and inhibits from clustering of metal ions.

To study the effect of Zn²⁺ ions adsorption on the electronic properties of P₄, the HOMO, and LUMO energies were obtained using optimization and NBO calculations. According to Table 1, the HOMO and LUMO energies of P₄ have been strongly decreased after the

chemisorption of Zn²⁺ ions into cavities of this molecule. Also, the E_g of P₄ has been increased from 0.95 to 1.40 eV ($\% \Delta E_g$ about 47%) with the chemisorption of Zn²⁺ metal ions into cavities of P₄. Furthermore, a major change was observed in the proximity of Fermi level in the DOS plot of the Zn4P₄ system (Fig. 1). Such changes showed that owing to this chemisorption, the E_g of Zn4P₄ system has increased significantly. Consequently, the electrical conductivity (σ) is expected to decrease. As a result of the positive ΔN value (Table 1), electrons have flowed from a definitely occupied orbital of P₄ into a definite empty orbital on Zn²⁺ metal ions.

In quantum chemistry, a bimolecular interaction is described by the Frontier Orbitals Theory (FOT) [26, 27]. Our calculations indicated that the energy span between the HOMO_{Zn4P4} and the LUMO_{P4} was 16.37 eV. While the energy span between the LUMO_{Zn4P4} and the HOMO_{P4} was 14.01 eV (Table 1). According to FOT, the smaller value is favorable and belongs to the interaction which occurs mainly between the HOMO_{P4} and the LUMO_{Zn4P4}. These results are in agreement with the calculated ΔN .

However, during the chemisorption of Zn²⁺ ions into porphyrin cavities, the bond lengths of C-C in methine bridges and butadiyne linkages display shorter values while the C-N bonds of pyrroles show longer values (Fig. 1). Such change could be due to the weakening of π interactions between ring atoms after the formation of the metal complex and this is in consistent with electron transfer to metal.

The electric dipole moment vector of species is an important property that shows the charge distribution in the system. The dipole moments of P₄, Zn4P₄ with symmetrical structures are approximately equal to zero (Table 1). As shown in Table 1, the Φ value of Zn4P₄ is about 3.19 eV.

The calculated values of molecular quantum descriptors including ω , S, η , and μ in the gas phase for Zn4P₄ compounds were reported in Table 2. The values of S and η for Zn4P₄ were 0.70 and 0.71 eV, respectively. This evidence indicated that the Zn4P₄ is a weak electrophile with high chemical activity.

Effects of CO gas molecule adsorption on Zn4P₄

We have found that in CAM-B3LYP/6-31G (d,p) level of theory the C-O bond length in CO is 1.137 Å. This fact is in agreement with previous studies [28].

Table 1: BSSE corrected adsorption energy (E_{ads}^{BSSE}), equilibrium distance ($R_{gas/Zn}$), HOMO and LUMO energy, the energy of Fermi level (E_{FL}), energy difference of HOMO and LUMO orbitals (band gap; E_g), the electron transfer number (ΔN) and dipole moment (DM) work function (Φ).

Systems	CO	P ₄	Zn4P4
E_{ads}^{BSSE} (eV)	-	-	-229.10
E_{HOMO} (eV)	-6.81	10.82	-4.59
E_{FL} (eV)	-5.84	11.30	-3.89
E_{LUMO} (eV)	-4.88	11.78	-3.19
E_g (eV)	1.93	0.95	1.40
$\% \Delta E_g$	-	-	47.37
DM(debye)	0.00	0.00	0.00
ΔN	-	-	0.82
Φ (eV)	5.84	-11.30	3.19

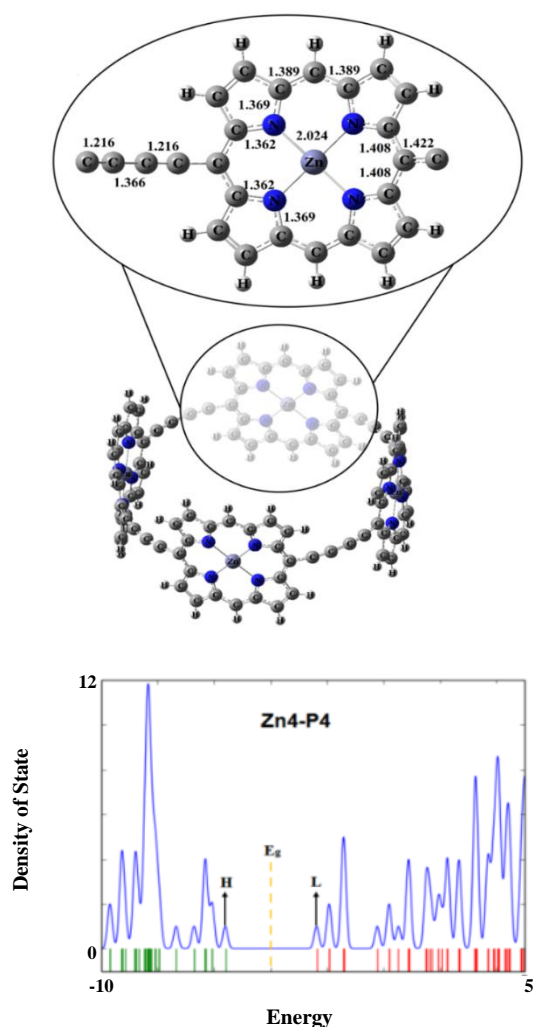


Fig. 1: The optimized structures and bond length (\AA) obtained at CAM-B3LYP/6-31G (d,p) level for P₄, Zn4P4 .

Generally, by adsorption of gas molecules on Zn4P4, near the adsorption place, the length of Zn-N and also C-C in methine bridges increased while the bond length of C-C in butadiyne linkage and C-N in pyrrole rings decreased (Figs. 1-3).

During the adsorption of CO gas molecule on Zn4P4 the symmetry of this nonpolar system is disturbed and so, the dipole moments increase considerably (Tables 1 and 3).

Effects of CO molecule adsorption on Zn4P4

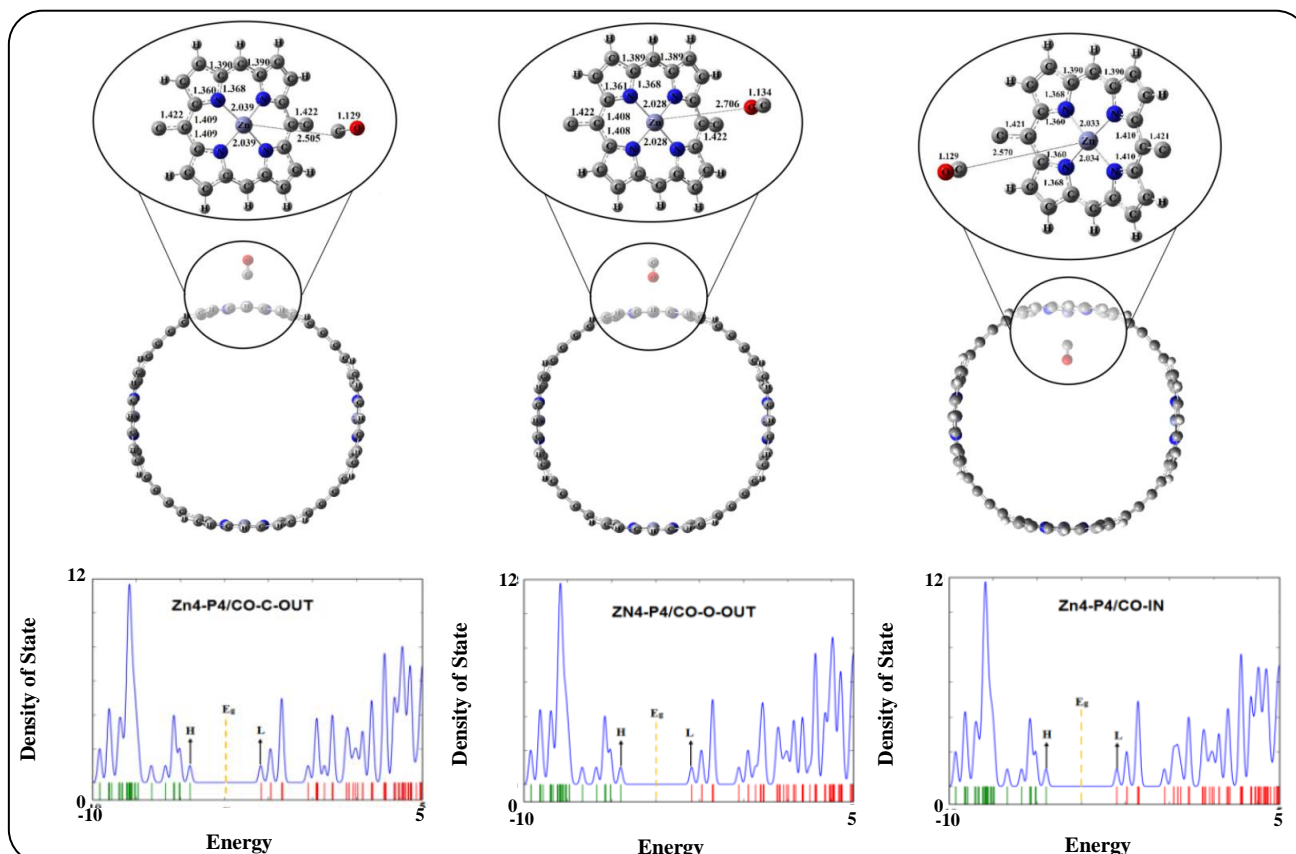
The optimized structures of CO adsorption on Zn4P4 compound were shown in Fig. 2. Obviously, in Zn4P4, the CO gas molecules have interaction with Zn^{+2} ions from inside or outside of the nanoring.

The optimization results and counterpoise corrected calculations showed that the E_{ads}^{BSSE} values were negative for CO interaction with Zn4P4 which indicated that the adsorption process was exothermic and favorable in standard temperature and pressure (Table 3).

Here it should be remarked that the adsorption of CO gas molecule on Zn4P4 nanoring from the outer side is higher than the inner side. Moreover, the adsorption from the Carbon site of CO gas molecule is stronger than from the Oxygen site. Also, the closest distance of CO with Zn4P4 molecule is in the range of 2.505-2.706 Å. Moreover, the range of E_{ads}^{BSSE} values were from -6.50 to -9.40 kCal/mol. The results revealed that during the adsorption of CO gas molecule on Zn4P4 the amounts of E_g and consequently, σ have been considerably changed.

Table 2: Chemical potential (μ), hardness (η), softness (S), and electrophilicity (ω) of Zn4P4 and Zn4P4-T₆.

Systems	μ (eV)	η (eV)	S (1/eV)	ω (eV)
CO	-5.84	0.96	0.52	17.70
Zn4P4	-3.90	0.71	0.70	10.81

**Fig. 2: The optimized structure, bond length (Å), and DOS plots obtained at CAM-B3LYP/6-31G (d,p) level for CO adsorption on Zn4P4.**

Also, it was found that as a result of CO adsorption, through all configurations, on Zn4P4 the DOS plots have been significantly changed in near the Fermi level. Furthermore, the amount of ΔN shows that the minor electron flow is directed from HOMO of Zn4P4 into LUMO of CO gas molecule. As a result, it is expected that the Zn4P4 could be a promising nominee in gas sensor design for the detection of CO gas. According to this evidence, all the adsorption process was physisorption and so, could be suitable candidates for CO sensing.

According to Tables 1-3, significant changes in the values of Φ and molecular quantum descriptors were observed. It means that CO molecule adsorption has a considerable effect on the field emission properties of Zn4P4 nanoring.

Effect of simultaneous adsorption of two CO gas molecules on Zn4P4

The adsorption configurations of two CO molecules in ortho-like (2CO-ORTHO), para-like (2CO-PARA), and 2CO-IN-OUT positions on the Zn4P4 nanoring were considered. The optimized structures of these three adsorption configurations were shown in Fig. 3.

The structural studies showed similar results to the way that one CO molecule approach. By approaching two CO molecules, the C-O bond length decreased after adsorption on Zn4P4 from 1.137 to 1.131 Å . However, there was a considerable change in the structural properties of Zn4P4 nanoring.

As can be seen in Table 3, by simultaneous adsorption of two CO gas molecules on Zn4P4, in ortho and para like

Table 3: BSSE corrected adsorption energy (E_{ads}^{BSSE}), HOMO and LUMO energy, energy of Fermi level (E_{FL}), energy difference of HOMO and LUMO orbitals (band gap; E_g), the electron transfer number (ΔN) and dipole moment (DM) work function (Φ).

Zn4P4						
Systems	CO-IN-C	CO-OUT-C	CO-OUT-O	2CO-IN-OUT	2CO-ORTHO	2CO-PARA
E_{ads}^{BSSE} (kCal/mol)	-9.1	-9.4	-6.5	-14.7	-17.7	-17.7
E_{HOMO} (eV)	-5.51	-5.48	-5.49	-5.47	-5.44	-5.45
E_{FL} (eV)	-1.2	-1.18	-1.19	-1.19	-1.17	-1.17
E_{LUMO} (eV)	-2.4	-2.37	-2.37	-2.38	-2.34	-2.34
E_g (eV)	3.1	3.11	3.11	3.09	3.1	3.1
$\% \Delta E_g$	121.76	122.38	122.81	120.75	121.62	121.66
ΔN	0.09	0.11	0.09	0.09	0.09	0.09
DM (Debye)	0.85	1.7	1.46	0.65	2.43	0.01
Φ (eV)	1.2	1.18	1.19	1.19	1.17	1.17
$\% \Delta \Phi$ (eV)	-69.11	-69.52	-69.5	-69.35	-69.87	-69.87

adsorption configurations, the E_{ads}^{BSSE} has been increased nearly two times (about -17.70 kCal/mol) than the state that one CO gas molecule approaches (-9.40 kCal/mol). Although, in Zn4P4-2CO-IN-OUT adsorption configuration, the E_{ads}^{BSSE} has been increasingly less than two times (about -14.70 kCal/mol) relative to the state that one CO gas molecule approaches. This is due to the fact that the adsorption of CO gas from the exterior site is stronger than the inner surface of nanoring. In ortho/para-like adsorption configurations, the Zn4P4-2CO-IN-OUT two and one CO gas molecules are approached from the outer surface of nanorings, respectively.

However, the different positions of two CO molecules on Zn4P4 approximately have similar E_{ads}^{BSSE} values. According to this evidence, the all adsorption process was physisorption.

For all three 2CO adsorption configurations, the energy of HOMO and LUMO and their difference (E_g) was obtained using optimization calculations and DOS diagrams (Table 3 and Fig. 3). These values show equal HOMO and LUMO energies, as well as, E_g . According to the conductivity equation, the σ amount of Zn4P4 is expected to be constant for all three adsorption configurations. These results confirmed that the Zn4P4 nano ring is suitable as a sensor for CO gas molecules. Here, it should be highlighted that since the simultaneous approach of two CO molecules have no significant effect on E_g .

According to ($\tau = \nu_0^{-1} \exp(-E_{ads}^{BSSE}/K_B T)$) equation, the lower values of E_{ads}^{BSSE} in the physisorption process showed the more easily separation and short recycle time (τ) of CO gas molecule [29-30]. In this equation T, K_B and ν_0 were temperatures, Boltzmann's constant, and attempt frequency, respectively.

For the judgment of the recovery time, we have employed three attempt frequencies, viz., the frequency corresponding to IR light ($\sim 1 \times 10^{12}$ Hz), yellow light ($\sim 5.2 \times 10^{14}$ Hz), and the UV light ($\sim 1 \times 10^{16}$ Hz). Subsequently, the recovery time has been calculated at two different temperatures (300 and 500 K).

The values of recovery time calculated using the IR light (τ_I), yellow light (τ_Y), and UV light (τ_{UV}) are reported in Table 4. Obviously, the more negative adsorption energy corresponds to the higher recovery time. At 300 K temperature, all adsorption configurations record promising values of τ_I , τ_Y , and τ_{UV} . Here, it should be noted that at 500 K temperature, the recovery time of all systems further decreases as expected. However, by changing the attempt frequencies a significant improvement in the recovery time of all systems was observed. In another word, when UV light is applied, the recovery times show a further decrease than when other lights are used.

The molecular quantum descriptors values for adsorption configurations of CO on Zn4P4 were given in Table 5. The results showed that the CO gas adsorption has a noticeable effect on μ , ω , η , and S values of Zn4P4.

Table 4: Recovery time of CO adsorbed on the 4-Zn-porphyrin nanoring using IR, yellow and the UV light at temperatures 300 K and 500 K.

Orientation	Eads (kJ/mol)	Eads (kJ/mol) for each CO	T (K)	τ_1 (μ S)	τ_γ (nS)	τ_U (pS)
Zn4P4-CO-IN-C	-38.07	-38.07	300	4.2	8.1	423.1
			500	0.0	0.0	0.9
Zn4P4-CO-C-OUT	-39.33	-39.33	300	7.0	13.5	699.6
			500	0.0	0.0	1.3
Zn4P4-CO-O-OUT	-27.20	-27.20	300	0.1	0.1	5.4
			500	0.0	0.0	0.1
Zn4P4-2CO-IN-OUT	-61.50	-30.75	300	50602.7	97312.9	5060271.0
			500	2.6	5.1	264.5
Zn4P4-2CO-ORTHO	-74.06	-37.03	300	7739252.9	14883178.7	773925294.7
			500	54.1	104.0	5410.3
Zn4P4-2CO-PARA	-74.06	-37.03	300	7739252.9	14883178.7	773925294.7
			500	54.1	104.0	5410.3

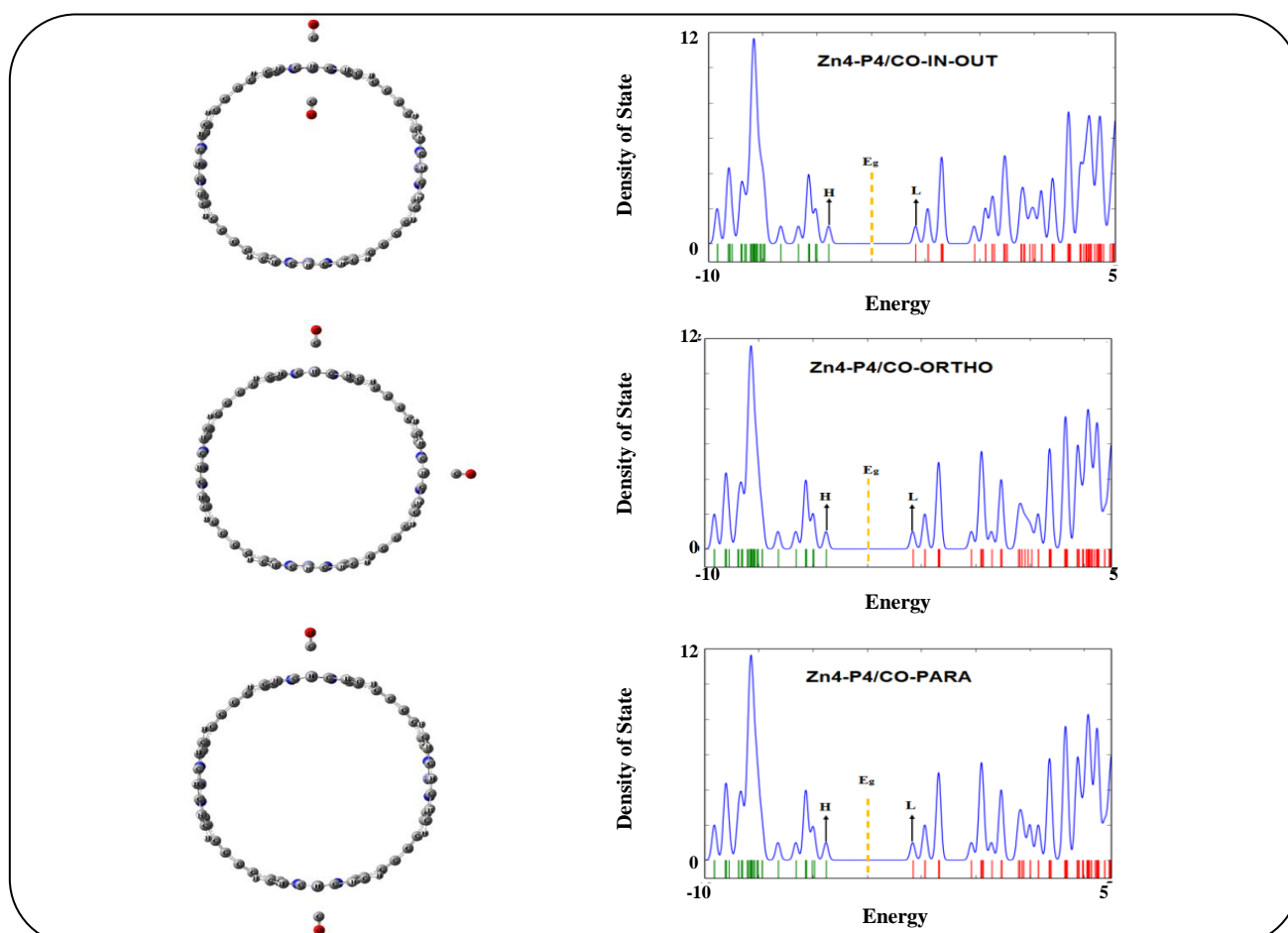


Fig. 3 The optimized structure and DOS plots obtained at CAM-B3LYP/6-31G (d,p) level for CO adsorption in ortho, para, and 2CO-IN-OUT orientation on Zn4P4.

Table 5: Chemical potential (μ), hardness (η), softness (S), and electrophilicity (ω) of CO adsorption configurations on Zn4P4.

Systems	Orientation	μ	η	S	ω
Zn4P4	CO-IN-C	-3.962	1.559	0.780	5.034
	CO-OUT-C	-3.952	1.563	0.782	5.022
	CO-OUT-O	-3.870	1.564	0.782	4.993
	2CO-IN-OUT	-3.954	1.559	0.780	4.803
	2CO-ORTHO	-3.958	1.565	0.782	4.995
	2CO-PARA	-3.890	1.564	0.782	5.008

Changes in molecular quantum descriptors values in the Zn4P4 confirm the greater ability of Zn4P4 in the identification and diagnosis of CO molecules [31].

The work function values of Zn4P4 (3.19eV) compound after adsorption of CO molecule, have been decreased to 1.20. A decrease of Φ makes field emission properties of Zn4P4 compound and the separation of electrons from their surface easier and decreases the electron affinity.

The calculated ΔN values show that the direction of electron flow is from HOMO of Zn4P4 into LUMO of CO gas molecules. To study the direction of electron flow, the frontier orbitals of Zn4P4CO systems were investigated. The results showed that the energy span between HOMO_{Zn4P4} and LUMO_{CO} gas molecules is smaller than the energy difference between HOMO_{CO} and LUMO_{Zn4P4}. According to the points, it was found that the electron flow direction is from HOMO_{Zn4P4} to LUMO_{CO} which are in agreement with ΔN values inserted in Table 3.

Generally, by adsorption of gas molecules on Zn4P4, the bond length of CO decreased. This fact was confirmed by the greater value of ΔN from Zn4P4 to CO gas molecule.

Natural population analysis: Donor-acceptor interactions

The natural bond orbital analysis is one of many available options for 'translating' computational solutions of a given wave function into localized form, corresponding to the two-center (bonds) and one-center (lone pairs) elements of the Lewis structure. The NBO analysis provides an efficient method for studying inter and intramolecular bonding and interaction among bonds and also provides a convenient basis for the investigation of charge transfer or conjugative interactions in the molecular system [32]. In NBO analysis, the input atomic orbital basis set is transformed *via* Natural Atomic Orbitals (NAOs) and Natural Hybrid Orbitals (NHOs) into NBOs [33].

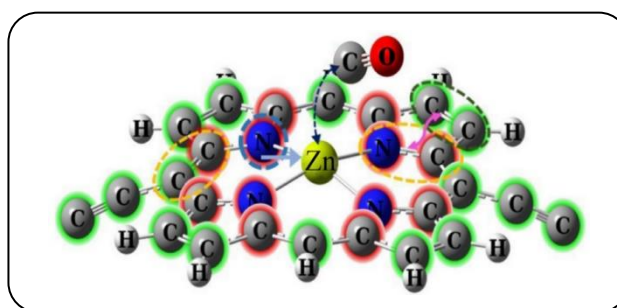


Fig. 4: Schematic presentation of various stabilization energy interactions of donor-acceptor orbitals for Zn4P4-CO systems.

The NBO was developed by Winhold [34]. The stabilization energy related to i - j transfer is estimated from $E^{(2)} = \Delta E_{ij} = q_i(F(i,j)^2/\epsilon_j - \epsilon_i)$ equation. In this equation, q_i is the occupied number of donor orbital, $F(i,j)$ are non-diagonal elements, and ϵ_i, ϵ_j are diagonal elements of the Fock matrix.

The NBO calculations were performed in order to understand various interactions between the (donor) Lewis-type NBOs and empty (acceptor) non-Lewis NBOs. The stabilization energies (E^2) of the most important interactions between electron-donor orbitals (i) and electron-acceptor orbitals (j) in P₄, Zn4P4 systems was given in Table 6 and Fig. 4.

The most important interactions in P₄, Zn4P4, and Zn4P4-CO as shown in Fig. 4, are:

$$\begin{aligned} & \sum \left(\pi_{(C-C)}^{\text{Donor}} \rightarrow \pi_{(C-N)}^{\text{*Acceptor}} \right), \quad \sum \left(\pi_{(C-N)}^{\text{Donor}} \rightarrow \pi_{(C-C)}^{\text{*Acceptor}} \right), \\ & \sum \left(LP_{(N)}^{\text{Donor}} \rightarrow \pi_{(C-C)}^{\text{*Acceptor}} \right), \quad \sum \left(LP_{(N)}^{\text{Donor}} \rightarrow LP_{(Zn)}^{\text{*Acceptor}} \right), \\ & \text{and } \sum \left(LP_{(C)}^{\text{Donor}} \rightarrow LP_{(Zn)}^{\text{*Acceptor}} \right). \end{aligned}$$

The two equal delocalization in P₄:

$$\sum E^2 \left(\pi_{(C-C)}^{\text{Donor}} \rightarrow \pi_{(C-N)}^{\text{*Acceptor}} \right) \cong \sum E^2 \left(\pi_{(C-N)}^{\text{Donor}} \rightarrow \pi_{(C-C)}^{\text{*Acceptor}} \right)$$

causes a monotone distribution of π electrons in this nanoring.

Table 6: The calculated stabilization energies of donor-acceptor orbitals for P4, Zn4P4 –CO-OUT-C systems.

Donor (i)→ Acceptor (j)	P4 (kCal/mol)	Zn4P4 (kCal/mol)	Zn4P4 - CO-OUT-C (kCal/mol)
$\sum E^2 (\pi_{C-C}^{donor} \rightarrow \pi_{C-N}^{*donor})$	109.82	252.00	30.02
$\sum E^2 (\pi_{C-N}^{donor} \rightarrow \pi_{C-C}^{*donor})$	110.27	157.01	22.04
$\sum E^2 (LP_{(N)}^{donor} \rightarrow \pi_{C-C}^{*donor})$	32.54	43.45	139.12
$\sum E^2 (LP_{(N)}^{donor} \rightarrow LP_{Zn}^{*donor})$	–	227.02	144.90
$\sum E^2 (LP_{(C)}^{donor} \rightarrow LP_{Zn}^{*donor})$	–	–	26.05

In Zn4P4 the stabilization energy order of interactions are $\sum E^2 (\pi_{(C-C)}^{Donor} \rightarrow \pi_{(C-N)}^{*Acceptor}) > \sum E^2 (\pi_{(C-N)}^{Donor} \rightarrow \pi_{(C-C)}^{*Acceptor})$ as well as

$$\sum E^2 (LP_{(N)}^{Donor} \rightarrow LP_{(Zn)}^{*Acceptor}) > \sum E^2 (LP_{(N)}^{Donor} \rightarrow \pi_{(C-C)}^{*Acceptor}).$$

These facts lead to electron current from C to N atoms and also, from N to Zn in Zn4P4 Structure.

The study of interactions in the adsorbed state, Zn4P4-CO, indicates that the interactions are as follows:

$$\sum E^2 (\pi_{(C-C)}^{Donor} \rightarrow \pi_{(C-N)}^{*Acceptor}) > \sum E^2 (\pi_{(C-N)}^{Donor} \rightarrow \pi_{(C-C)}^{*Acceptor})$$

and

$$\sum E^2 (LP_{(N)}^{Donor} \rightarrow LP_{(Zn)}^{*Acceptor}) > \sum E^2 (LP_{(N)}^{Donor} \rightarrow \pi_{(C-C)}^{*Acceptor})$$

Undoubtedly, this phenomenon revealed that the delocalized electrons were transferred remarkably from C and N atoms to CO gas molecules through Zn bridge.

Also, the interaction $\sum E^2 (LP_{(O)}^{Donor} \rightarrow LP_{(Zn)}^{*Acceptor})$ leads to the backward transfer of a few electrons from O atom of CO molecule to Zn atom.

This work and other research showed that the nanostructures play the main role in the sensing ability and synthesis of organic compounds [35-84]

CONCLUSIONS

In this study, the DFT calculations were used at CAM-B3LYP/6-31G (d,p) level of theory to scrutinize the CO sensing ability of Zn4P4 nanoring.

Geometrical structures, electronic properties, binding energies, ΔN , FOM, DOS, distribution of the HOMO-LUMO, and NBO basis analysis were scrutinized. The Zn4P4 nanorings, however, showed significant electrical variation with CO adsorption. During the CO adsorption, the cavity size in Zn4P4 will be increased and conjugated

atoms of nanorings transfer charge to CO gas via nitrogen porphyrin-Zn bridge and increase the negative charge on its surface.

The amount of E_g has been considerably increased with adsorption of CO gas molecule on Zn4P4. Based on calculated E_{ads}^{BSSE} and $\% \Delta E_g$, it is expected that the new electric sensor could be a promising candidate for the detection of CO with fast response. Simultaneous adsorption of two CO gas molecules on Zn4P4, in ortho and para-like adsorption configurations, the E_{ads}^{BSSE} has been increased nearly two times than the state that one CO gas molecule approaches. However, the different positions of two CO molecules on Zn4P4 approximately have similar E_{ads}^{BSSE} values

Acknowledgments

The authors gratefully acknowledge the support of this work by Payame Noor University. Also, we especially thank Dr. M. Salary, for her suggestions and cordial cooperation.

Received : Mar. 15, 2022 ; Accepted : Apr. 25, 2022

REFERENCE

- [1] Mohajeri S., Kamani M., Salari A.A., Noei M., Ebrahimikia M., Ahmadaghaei N., Molaei N., *Adsorption of Aniline Toxic Gas on a BeO Nanotube, Iran. J. Chem. Chem. Eng.(IJCCE)*, **38(1)**: 43-48 (2019).
- [2] Aratani N., Kim D., Osuka A., *Discrete Cyclic Porphyrin Arrays as Artificial Light-Harvesting Antenna, Accounts of Chemical Research*, **42(12)**: 1922-1934 (2009).
- [3] Collman J. P., Fu L., *Synthetic Models for Hemoglobin and Myoglobin, Accounts of Chemical Research*, **32(6)**: 455-463 (1999).
- [4] Taylor P., Aplin R., Anderson H., *Conjugated Porphyrin Oligomers from Monomer to Hexamer, Chemical Communications*, **(8)**: 909-910 (1998).

- [5] Screen T.E., Thorne J.R., Denning R.G., Bucknall D.G., Anderson H. L., **Amplified Optical Nonlinearity in a Self-Assembled Double-Strand Conjugated Porphyrin Polymer Ladder**, *Journal of the American Chemical Society*, **124(33)**: 9712-9713(2002).
- [6] Posligua V., Aziz A., Haver R., Peeks M.D., Anderson H.L., Grau-Crespo R., **Band Structures of Periodic Porphyrin Nanostructures**, *The Journal of Physical Chemistry C*, **122(41)**: 23790-23798 (2018).
- [7] Rousseaux S.A., Gong J.Q., Haver R., Odell B., Claridge T.D., Herz L.M., Anderson H.L., **Self-Assembly of Russian Doll Concentric Porphyrin Nanorings**, *J. Am. Chem. Soc.* **137**:12713-12718 (2015).
- [8] Nakamura Y., Aratani N., Shinokubo H., Takagi A., Kawai T., Matsumoto T., Yoon Z.S., Kim D.Y., Ahn T.K., Kim D., Muranaka A., Kobayashi N., Osuka A., **A Directly Fused Tetrameric Porphyrin Sheet and Its Anomalous Electronic Properties that Arise from the Planar Cyclooctatetraene Core**, *J. Am. Chem. Soc.*, **128(12)**: 4119-4127 (2006).
- [9] Cremers J., Haver R., Rickhaus M., Gong J.Q., Favereau L., Peeks M.D., Claridge T.D.W., Herz L.M., Anderson H.L., **Template-Directed Synthesis of a Conjugated Zinc Porphyrin Nanoball**, *J. Am. Chem. Soc.*, **140(16)**:5352-5355 (2018).
- [10] Bressan G., Jirasek M., Anderson H.L., Heisler I.A., Meech S.R., **Exciton-Exciton Annihilation as a Probe of Exciton Diffusion in Large Porphyrin Nanorings**, *The Journal of Physical Chemistry C*, **124(34)**: 18416-18425 (2020).
- [11] O'Sullivan M.C., Sprafke J.K., Kondratuk D.V., Rinfray C., Claridge T.D., Saywell A., Anderson H.L., **Vernier Templating and Synthesis of a 12-Porphyrin Nano-Ring**, *Nature*, **469(7328)**: 72-75 (2011).
- [12] Richert S., Cremers J., Anderson H.L., Timmel C.R., **Exploring Template-Bound Dinuclear Copper Porphyrin Nanorings by EPR Spectroscopy**, *Chemical Science*, **7(12)**: 6952-6960 (2016).
- [13] Fukui K., **The Role of Frontier Orbitals in Chemical Reactions (Nobel Lecture)**, *Angewandte Chemie International Edition in English*, **21(11)**: 801-809 (1982).
- [14] Reed A.E., Curtiss L.A., Weinhold F., **Intermolecular Interactions from a Natural Bond Orbital, Donor-Acceptor Viewpoint**, *Chemical Reviews*, **88(6)**: 899-926 (1988).
<https://doi.org/10.1021/cr00088a005>
- [15] Asgari Y., Ghaemi M., Mahjani M., **Cellular Automata Simulation of a Bistable Reaction-Diffusion System: Microscopic and Macroscopic Approaches**, *Iran. J. Chem. Chem. Eng. (IJCCE)*, **30(1)**: 143-150 (2011).
<https://doi.org/10.30492/ijcce.2011.6366>
- [16] Pirsa S., Zandi M., Almasi H., Hasanlu S., **Selective Hydrogen Peroxide Gas Sensor Based on Nanosized Polypyrrole Modified by CuO Nanoparticles**, *Sensor Letters*, **13(7)**: 578-583 (2015).
- [17] Schmidt M.W., Baldrige K.K., Boatz J.A., Elbert S.T., Gordon M. S., Jensen J.H., Koseki S., Matsunaga N., Nguyen K.A., Su Sh., Windus T.L., Dupuis M., Montgomery Jr, J. A. **General Atomic and Molecular Electronic Structure System**, *Journal of Computational Chemistry*, **14(11)**: 1347-1363 (1993).
- [18] Saeidipoor A., Arshadi S., Benam M. R., **The Titano-Porphyrin Doped Pillared Graphene as a Novel "Turn-Off" Fluorescent Sensor for CO Gas: Theoretical Study**, *Physica E: Low-Dimensional Systems and Nanostructures*, **127**: 114554 (2021).
- [19] Arshadi S., Pourkhiz F., **NBO, AIM, and TD-DFT Assisted Screening of BNNT Optimum Diameter on Ethyl Phosphorodimethylamidocyanidate Sensor Design**, *Phosphorus, Sulfur, and Silicon and the Related Elements*, **191(7)**: 1013-1021 (2016).
<https://doi.org/10.1080/10426507.2015.1130045>
- [20] Pohle R., Tawil A., Davydovskaya P., Fleischer M., **Metal Organic Frameworks as Promising High Surface Area Material for Work Function Gas Sensors**, *Procedia Engineering*, **25**: 108-111 (2011).
- [21] Koopmans T., **Ordering of Wave Functions and Eigenenergies to the Individual Electrons of an Atom**. *Physica*, **1**: 104-113 (1933).
- [22] Parr R.G., Szentpály L.V., Liu S., **Electrophilicity Index**, *Journal of the American Chemical Society*, **121(9)**: 1922-1924 (1999).
- [23] Arshadi S., Anisheh F., **Theoretical Study of Cr and Co-Porphyrin-Induced C70 Fullerene: A Request for a Novel Sensor of Sulfur and Nitrogen Dioxide**, *Journal of Sulfur Chemistry*, **38(4)**: 357-371 (2017).
- [24] Brémond É.A., Kieffer J., Adamo C., **A Reliable Method for Fitting TD-DFT Transitions to Experimental UV-Visible Spectra**, *Journal of Molecular Structure: THEOCHEM*, **954(1-3)**: 52-56 (2010).
<https://doi.org/10.1016/j.chemphys.2004.09.020>

- [25] Al E.B., Kasapoglu E., Sakiroglu S., Sari H., Sökmen I., Duque C.A., **Binding Energies and Optical Absorption of Donor Impurities in Spherical Quantum Dot under Applied Magnetic Field**, *Physica E: Low-Dimensional Systems and Nanostructures*, **119**: 114011 (2020).
<https://doi.org/10.1016/j.physe.2020.114011>
- [26] Lu G., Yuan Y., Deng K., Wu H., Yang J., Wang X., **Density-Functional Energetics and Frontier Orbitals Analysis for the Derivatives of the Nonclassical Four-Membered Ring Fullerene C₆₂**, *Chemical Physics Letters*, **424(1-3)**: 142-145 (2006).
<https://doi.org/10.1016/j.cplett.2006.04.063>
- [27] Tang C., Zhu W., Deng K., **Density Functional Energetics and Frontier Orbitals Analysis for the Derivatives of the Nonclassical Triplet-Pentagon-Fusion Fullerene C₆₄X (X= Si And Ge)**, *Journal of Molecular Structure: THEOCHEM*, **950(1-3)**: 36-40 (2010).
<https://doi.org/10.1016/j.theochem.2010.03.019>
- [28] Shalabi A.S., Aal S.A., Kamel M.A., Taha H.O., Ammar H.Y., Halim W.A., **The Role of Oxidation States in FA1 Tln+ (N= 1, 3) Lasers and CO Interactions at the (1 0 0) Surface of NaCl: An Ab Initio Study**, *Chemical Physics*, **328(1-3)**: 8-16 (2006).
- [29] Olatunde A.O., Olafadehan O.A., Usman M.A., **Modeling and Simulation of Partial Oxidation of Methanol to Formaldehyde on FeO/MoO₃ Catalyst in a Catalytic Fixed Bed Reactor**, *Iran. J. Chem. Chem. Eng. (IJCCE)*, **40(6)**: 1800-1813 (2021).
- [30] Zhao Z., Yong Y., Zhou Q., Kuang Y., Li X., **Gas-sensing Properties of the SiC Monolayer and Bilayer: A Density Functional Theory Study**, *ACS Omega*, **5(21)**: 12364-12373 (2020).
- [31] Hosseini A., Salary M., Arshadi S., Vessally E., Edjlali L., **The Interaction of Phosgene Gas with Different BN Nanocones: DFT Studies**, *Solid State Communications*, **269**: 23-27 (2018).
- [32] Yong C.K., Parkinson P., Kondratuk D.V., Chen W.H., Stannard A., Summerfield A., Herz L.M., **Ultrafast Delocalization of Excitation in Synthetic Light-Harvesting Nanorings**, *Chemical Science*, **6(1)**: 181-189 (2015).
- [33] Glendening E.D., Landis C.R., Weinhold F., **Natural Bond Orbital Methods**, *Wiley Interdisciplinary Reviews: Computational Molecular Science*, **2(1)**: 1-42 (2012).
- [34] Weinhold F., Landis C.R., Glendening E.D., **What Is NBO Analysis and How Is It Useful?**, *Int. Rev. Phys. Chem.*, **35(3)**: 399-440 (2016).
- [35] Norouzi N., Talebi S., Shahbazi A., **An Overview on the Carbon Capture Technologies with an Approach of Green Coal Production Study**, *Chem. Rev. Lett.* **3**: 65-78 (2020).
<https://doi.org/10.22034/crl.2020.224177.1043>
- [36] Vessally E., Mohammadi S., Abdoli M., Hosseini A., Ojaghloo P., **Convenient and Robust Metal-Free Synthesis of Benzazole-2-ones through the Reaction of Aniline Derivatives and Sodium Cyanate in Aqueous Medium**, *Iran. J. Chem. Chem. Eng. (IJCCE)* **39(5)**: 11-19 (2020).
- [37] Gharibzadeh F., Vessally E., Edjlali L., Es'haghi M., Mohammadi R., **A DFT Study on Sumanene, Corannulene and Nanosheet as the Anodes in Li-Ion**, *Iran. J. Chem. Chem. Eng. (IJCCE)*, **39(6)**: 51-62 (2020).
- [38] Afshar M., Khojasteh R.R., Ahmadi R., Nakhaei Moghaddam M., **In Silico Adsorption of Lomustin Anticancer Drug on the Surface of Boron Nitride**, *Chem. Rev. Lett.* **4**: 178-184 (2021).
- [39] Norouzi N., **Future of Hydrogen in Energy Transition and Reform**, *J. Chem. Lett.*, **2**: 64-72 (2021).
[10.22034/jchemlett.2021.301002.1036](https://doi.org/10.22034/jchemlett.2021.301002.1036)
- [40] Vessally E., Hosseini A., **A Computational Study on the Some Small Graphene-Like Nanostructures as the Anodes in Na-Ion Batteries**, *Iran. J. Chem. Chem. Eng. (IJCCE)*, **40(3)**: 691-703 (2021).
- [41] Hashemzadeh, B., Edjlali L., Delir Kheirollahi Nezhad P., Vessally, E., **A DFT Studies on a Potential Anode Compound for Li-Ion Batteries: Hexa-cata-hexabenzocoronene Nanographen**, *Chem. Rev. Lett.*, **4**: 232-238 (2021).
<https://doi.org/10.22034/crl.2020.187273.1087>
- [42] Vessally E., Farajzadeh P., Najafi E., **Possible Sensing Ability of Boron Nitride Nanosheet and Its Al- and Si-Doped Derivatives for Methimazole Drug**, *Iran. J. Chem. Chem. Eng. (IJCCE)*, **40(3)**: 1001-1011 (2021).
- [43] Majedi S., Sreerama L., Vessally E., Behmagham F., **Metal-Free Regioselective Thiocyanation of (Hetero) Aromatic C-H Bonds using Ammonium Thiocyanate: An Overview**, *J. Chem. Lett.*, **1**: 25-31 (2020).
<https://doi.org/10.22034/jchemlett.2020.107760>

- [44] Amani V., Zakeri M., Ahmadi R. **Binuclear Nickel(II) Complex Containing 6-methyl-2,2'-bipyridine and Chloride Ligands: Synthesis, Characterization, Thermal Analyses, and Crystal**, *Iran. J. Chem. Chem. Eng. (IJCCE)*, **39(2)**: 113-122 (2020).
[10.30492/IJCCE.2020.33338](https://doi.org/10.30492/IJCCE.2020.33338)
- [45] Salehi N., Vessally E., Edjlali L., Alkorta I., Eshaghi M., **Nan@Tetracyanoethylene (n=1-4) Systems: Sodium Salt vs Sodium**, *Chem. Rev. Lett.*, **3**: 207-217 (2020).
<https://doi.org/10.22034/crl.2020.230543.1056>
- [46] Soleimani-Amiri S., Asadbeigi N., Badragheh S., **A Theoretical Approach to New Triplet and Quintet (nitrenoethynyl) alkylmethylenes,(nitrenoethynyl) alkylsilylenes,(nitrenoethynyl)** *Iran. J. Chem. Chem. Eng. (IJCCE)*, **39(4)**: 39-52 (2020).
[10.30492/IJCCE.2018.31990](https://doi.org/10.30492/IJCCE.2018.31990)
- [47] Sreerama L., Vessally E., Behmagham F., **Oxidative Lactamization of Amino Alcohols**: *J. Chem. Lett.*, **1**: 9-18 (2020).
[10.22034/jchemlett.2020.106645](https://doi.org/10.22034/jchemlett.2020.106645)
- [48] Norouzi N., Ebadi A.G., Bozorgian A., Vessally E., Hoseyni S.J., **Energy and Exergy Analysis of Internal Combustion Engine Performance of Spark Ignition for Gasoline, Methane, and Hydrogen Fuels**, *Iran. J. Chem. Chem. Eng. (IJCCE)*, **40(6)**: 1909-1930 (2021).
[10.30492/IJCCE.2022.539658.4948](https://doi.org/10.30492/IJCCE.2022.539658.4948)
- [49] Kamel M., Mohammadifard M., **Thermodynamic and Reactivity Descriptors Studies on the Interaction of Flutamide Anticancer Drug with Nucleobases: A Computational View**, *Chem. Rev. Lett.*, **4**: 54-65 (2021).
<https://doi.org/10.22034/crl.2020.259697.1093>
- [50] Vessally E., Musavi M., Poor Heravi M.R., **A Density Functional Theory Study of Adsorption Ethionamide on the Surface of the Pristine, Si and Ga and Al-Doped Graphene**, *Iran. J. Chem. Chem. Eng. (IJCCE)*, **40(6)**: 1720-1736 (2021).
[10.30492/IJCCE.2022.532176.4794](https://doi.org/10.30492/IJCCE.2022.532176.4794)
- [51] Vakili M., Bahramzadeh V., Vakili M., **A Comparative Study of SCN-Adsorption on the Al12N12, Al12P12, and Si and Ge -Doped Al12N12 Nano-Cages to Remove ...**, *J. Chem. Lett.*, **1**: 172-178 (2020).
[10.22034/jchemlett.2022.329629.1052](https://doi.org/10.22034/jchemlett.2022.329629.1052)
- [52] Bozorgian A., Norouzi N., Ebadi A.D., Hoseyni S.J., Vessally E., **Cogeneration System of Power, Cooling, and Hydrogen from Geothermal Energy: An Exergy Approach**, *Iran. J. Chem. Chem. Eng. (IJCCE)*, **41(2)**: 706-721 (2022).
- [53] Mosavi M., **Adsorption Behavior of Mephentermine on the Pristine and Si, Al, Ga- Doped Boron Nitride Nanosheets: DFT Studies**, *J. Chem. Lett.*, **1**: 164-171 (2020).
[10.22034/jchemlett.2022.330189.1057](https://doi.org/10.22034/jchemlett.2022.330189.1057)
- [54] Norouzi N., Joda F., **Exergy and Stabilization Design of a Fusion Power Plant and Its Waste Heat Recovery to Hydrogen**, *Iran. J. Chem. Chem. Eng. (IJCCE)*, **41** (2022). [in Press]
[10.30492/ijcce.2022.533732.4826](https://doi.org/10.30492/ijcce.2022.533732.4826).
- [55] Norouzi N., Talebi S., **An Overview on the Green Petroleum Production**, *Chem. Rev. Lett.* **3**: 38-52 (2020)
[10.22034/crl.2020.222515.1041](https://doi.org/10.22034/crl.2020.222515.1041)
- [56] Vessally E., Siadati S.A., Hosseinian A., Edjlali L. **Selective Sensing of Ozone and the Chemically Active Gaseous Species of the Troposphere by Using the C₂₀ Fullerene and Graphene Segment**, *Talanta*, **162**: 505-510 (2017).
- [57] Rabipour S., Mahmood E.A., Afsharkhas M. **A Review on the Cannabinoids Impacts**, *Chem. Rev. Lett.* **5** (2022).
[10.22034/crl.2022.349864.1175](https://doi.org/10.22034/crl.2022.349864.1175)
- [58] Siadati S.A., Vessally E., Hosseinian A., Edjlali L. **Possibility of Sensing, Adsorbing, and Destructing the Tabun-2D-skeletal (Tabun Nerve Agent) by C₂₀ Fullerene and Its Boron and Nitrogen-Doped Derivatives**. *Synthetic Metals*, **220**: 606-611 (2016).
- [59] Norouzi N., Talebi S., **Exergy, Economical and Environmental Analysis of a Natural Gas Direct Chemical Looping Carbon Capture and Formic Acid-Based Hydrogen Storage System**, *Iran. J. Chem. Chem. Eng. (IJCCE)*, **41** (2022) [in Press].
<https://doi.org/10.30492/ijcce.2021.528164.4669>
- [60] Norouzi N. **Dynamic Modeling of the Effect of Vehicle Hybridization Policy on Carbon Emission and Energy Consumption**, *J. Chem. Lett.*, **3**: 99-106 (2022).
[10.22034/jchemlett.2022.352806.1078](https://doi.org/10.22034/jchemlett.2022.352806.1078)
- [61] Rabipour S., Mahmood E.A., Afsharkhas M., **Medicinal Use of Marijuana and Its Impacts on Respiratory System**, *J. Chem. Lett.* **3**: 86-94 (2022).
- [62] Norouzi N., Fani M., **Energy and Exergy Analysis and Selection of the Appropriate Operating Fluid for a Combined Power and Hydrogen Production System Using a Geothermal Fueled ORC and a PEM Electrolyzer**, *Iran. J. Chem. Chem. Eng. (IJCCE)*, **41** (2022) [in Press].
<https://doi.org/10.30492/ijcce.2021.530629.4739>

- [63] Cao Y., Soleimani-Amiri S., Ahmadi R., Issakhov A., Ebadi, A.G., Vessally, E., [Alkoxy-sulfonylation of Alkenes: Development and Recent Advances](#), *RSC Advances*, **11**: 32513-32525 (2021).
- [64] Vessally E., Soleimani-Amiri S., Hosseinian A., Edjlali, L., Babazadeh, M., [Chemical fixation of CO₂ to 2-aminobenzonitriles: A Straightforward Route to quinazoline-2, 4 \(1H, 3H\)-diones with Green and Sustainable](#), *J. CO₂ Util.* **21**: 342-352 (2017).
- [65] Arshadi S., Vessally E., Hosseinian A., Soleimani-Amiri S., Edjlali L. [Three-Component Coupling of CO₂, Propargyl Alcohols, and Amines: An Environmentally Benign Access to Cyclic and Acyclic Carbamates](#). *J. CO₂ Util.*, **21**: 108-118 (2017).
- [66] Kassae M.Z., Buazar F., Soleimani-Amiri S. [Triplet Germynes with Separable Minima at AB Initio and DFT Levels](#). *Journal of Molecular Structure*, **866(1-3)**: 52-57 (2008).
- [67] Kassae M.Z., Aref Rad H., Soleimani Amiri, S. [Carbon–Nitrogen Nanorings and Nanoribbons: A Theoretical Approach for Altering the Ground States of Cyclacenes and Polyacenes](#). *Monatshefte für Chemie-Chemical Monthly*, **141(12)**: 1313-1319 (2010).
- [68] Koochi M., Soleimani Amiri S., Haerizade B.N., [Substituent Effect on Structure, Stability, and Aromaticity of Novel BnNmC₂₀–\(n+m\) Heterofullerenes](#). *Journal of Physical Organic Chemistry*, **30(11)**: e3682 (2017).
- [69] Soleimani-Amiri S. [Singlet and Triplet Cyclonona-3, 5, 7-trienylidenes and Their \$\alpha\$, \$\alpha'\$ -halogenated Derivatives](#) *J. Phys. Org. Chem.*, **33(2)**: e4018 (2020).
- [70] Soleimani-Amiri S. [Identification of Structural, Spectroscopic, and Electronic Analysis of ...](#), *Polycycl. Aromat. Comp.*, **41(3)**: 635-652 (2021).
- [71] Poor Heravi M.R., Azizi B., Abdulkareem Mahmood E., Ebadi A.G., Ansari M.J., Soleimani-Amiri S. [Molecular Simulation of the Paracetamol Drug Interaction with Pt-decorated BC₃ Graphene-Like](#), *Molecular Simulation*, **48(6)**: 517-525 (2022).
- [72] Soleimani Amiri S. [Green Production and Antioxidant Activity Study of New Isoquinolines](#). *J. Heterocyclic Chem.*, **57(11)**: 4057-4069 (2020).
- [73] Samiei Z., Soleimani-Amiri S., Azizi Z. [Fe₃O₄@C@OSO₃H as an Efficient, Recyclable Magnetic Nanocatalyst in Pechmann Condensation: Green Synthesis](#), *Molecular Diversity*, **25(1)**: 67-86 (2021).
- [74] Soleimani-Amiri S., Ghazvini M., Khandan S., Afrashteh S. [KF/Clinoptilolite@MWCNTs Nanocomposites Promoted a Novel Four-Component Reaction of Isocyanides for the Green Synthesis](#). *Polycycl. Aromat. Comp*: 1-16 (2021).
- [75] Feizpour Bonab M., Soleimani-Amiri S., Mirza B., [Fe₃O₄@C@PrS-SO₃H: A Novel Efficient Magnetically Recoverable Heterogeneous Catalyst](#). *Polycycl. Aromat. Comp*: 1-16 (2022).
- [76] Khoshtarkib Z., Ebadi A., Alizadeh R., Ahmadi R., Amani V., [Dichloridobis \(phenanthridine- \$\kappa\$ N\) zinc \(II\)](#). *Acta Crystallographica Section E: Structure Reports Online*, **65(7)**: m739-m740 (2009).
- [77] Amani V., Ahmadi R., Naseh M., Ebadi A. [Synthesis, Spectroscopic Characterization, Crystal Structure and Thermal Analyses of ...](#) *Journal of the Iranian Chemical Society*, **14(3)**: 635-642 (2017).
- [78] Ahmadi R., Khalighi A., Kalateh K., Amani V., Khavasi H.R. [Catenated-Poly \[\(5, 5'-dimethyl-2, 2'-bipyridine- \$\kappa\$ 2N, N'\) cadmium \(II\)\]-di- \$\mu\$ -chlorido\]](#). *Acta Crystallographica Section E: Structure Reports Online*, **64(10)**: m1233-m1233 (2008).
- [79] Kadhim M.M., Mahmood E.A., Abbasi V., Poor Heravi M.R., Habibzadeh S., Mohammadi-Aghdam S., Shoaie S.M., [Theoretical Investigation of the Titanium–Nitrogen Heterofullerenes Evolved from the Smallest Fullerene](#), *J. Mol. Graph. Model.*, (2022). <https://doi.org/10.1016/j.jmkgm.2022.108269>.
- [80] Hosseini S.M., Hosseini-Monfared H., Abbasi V., [Silver Ferrite–Graphene Nanocomposite and Its Good Photocatalytic Performance in Air and Visible...](#), *Applied Organometallic Chemistry*, **31(4)**: e3589 (2017).
- [81] Abbasi V., Hosseini-Monfared H., Hosseini S.M., [Mn \(III\)- Salan/Graphene Oxide/Magnetite Nanocomposite as a Highly Selective Catalyst for Aerobic Epoxidation of Olefins](#), *Applied Organometallic Chemistry*, **31(2)**:e3554 (2017).
- [82] Abbasi V, Hosseini-Monfared H, Hosseini S.M., [A Heterogenized Chiral Imino Indanol Complex of Manganese as an Efficient Catalyst for Aerobic Epoxidation of Olefins](#), *New Journal of Chemistry*, **41(18)**: 9866-9874 (2017).
- [83] Hosseini S.M., Hosseini-Monfared H., Abbasi V., Khoshroo M.R., [Selective Oxidation of Hydrocarbons under Ar Using Recoverable Silver Ferrite–Graphene \(AgFeO₂–G\) Nanocomposite: A Good Catalyst for Green ...](#), *Inorg. Chem. Comm.* **67**:72-79 (2016).

- [84] Hosseini Monfared H, Abbasi V, Rezaei A, Ghorbanloo M, Aghaei A, [A Heterogenized Vanadium Oxo-arylhydrazone Catalyst for Efficient and Peroxide...](#), *Transition Metal Chemistry*, **37(1)**:85-92 (2012).